Progress in Fractional Differentiation and Applications
An International Journal

http://dx.doi.org/10.18576/pfda/110201

Study of COVID-19 SEWIR Model with Memory Effect of Fractal Derivative on Infectious Reaction Outbreak

Muhammad Farman[1,2,7], *Ali Akgül*[2,3,*], *Faisal Alshowaikh*[4], *Mohamed Hafez*[5], *Shawkat Alkhazaleh*[6], *Abdul Sattar Ghaffari*[7], *Evren Hincal*[1], *Kottakkaran Sooppy Nisar*[8], *and Hira Asif*[7]

[1] Faculty of Arts and Science, Department of Mathematics, Near East University, Turkey
[2] Department of Computer Science and Mathematics, Lebanese American University, Beirut, Lebanon
[3] Faculty of Arts and Science, Department of Mathematics, Siirt University, 56100 Siirt, Turkey
[4] Department of Mathematical Sciences, College of Arts and Science, Ahlia University, 10878. Manama. Kingdom of Bahrain
[5] Faculty of Engineering and Quantity Surviving, INTI International University Colleges, Nilai, Malaysia
[6] Department of Mathematics, Faculty of Sciences, Jadara University, Jordan
[7] Institute of Mathematics, Khawaja Fareed University of Engineering and Information Technology, Rahim Yar Khan 64200, Pakistan
[8] Department of Mathematics, College of Arts and Sciences, Wadi Aldawaser, 11991, Prince Sattam bin Abdulaziz University, Saudi Arabia

Received: 7 Nov. 2024, Revised: 24 Dec. 2024, Accepted: 26 Jan. 2025
Published online: 1 Apr. 2025

Abstract: The COVID-19 epidemic was a significant occurrence that had a significant influence on the global economic and health care systems. Machine learning techniques and mathematical models are being used to study the behaviour of the virus and make long and short term forecasts about the daily new cases. In this work, we construct a SEWIR epidemic model in this paper using the Mittag Lefler Kernel in terms of fractal fractional operator. The control rate and infectious force in this model are at their peak during the latent phase. We demonstrate the presence and originality of solutions and determine the model's fundamental reproductive number R_0. For the first and second derivative tests, a global stability investigation is started using the Lyapunov function. Quantitative analysis of the collapse of second derivative equilibrium points to demonstrate the impact of another wave of dynamical transmission. The model's parameters are subjected to sensitivity analysis in order to the specific factors with the greatest effects on the propagation rate. Infections point analysis was thoroughly explained, and a Mittag Lefler Kernel-based mathematical framework was used to develop the model's numerical solution.

Keywords: COVID-19 Model, Mittg Leffler Kernel, Lyapunov Stability, Unique Solution, Biological feasibility; Existence

1 Introduction

COVID-19, also known as the novel coronavirus, has had far-reaching impacts globally, affecting various aspects of society, such as health, the economy, education, and more. In terms of health impacts, COVID-19 has been associated with significant morbidity and mortality, with millions of confirmed cases and hundreds of thousands of deaths reported worldwide. A systematic review of 30 studies conducted [1] found that COVID-19 is associated with an increased risk of hospitalization and death, particularly in older adults and those with underlying medical conditions. The COVID-19 pandemic has also had significant economic impacts, with widespread job losses, declining business activity, and decreased consumer spending. According to [2], the pandemic has led to the worst economic downturn since the Great Depression. A study by [3] found that the COVID-19 pandemic has led to a significant decline in global trade and that the largest impact has been on the service sector. Moreover, the pandemic has disrupted education, with schools and universities closing globally, leading to widespread shifts to remote learning. A study by [4] found that the shift to remote learning has had negative impacts on student learning and has widened existing disparities in education. It is clear that COVID-19 has had widespread impacts on various aspects of society, and it will continue to shape our world in the coming years. In epidemiology, the SEIR model is frequently employed. The entire group is divided into four sections: vulnerable,

* Corresponding author e-mail: aliakgul00727@gmail.com

exposed, infected and recovered. Early on in their studies, many researchers took into account fewer variables, and the majority of them employed the SEIR model directly to investigate and evaluate epidemic illnesses [5]. An SEIR epidemic model like the one mentioned in [5] was examined by Carcione et al. in [6]. By replacing the control values for the four populations, the pace at which exposure leads to disease, and the infected population's recapture rate, they were able to duplicate the infection and mortality curves. It was confirmed how crucial and successful isolation and medical level were in halting the virus's transmission [5,6].

Fractal fractional calculus (FFC) is an area of mathematics that studies the fractional derivatives of fractal functions. It combines the ideas of fractional calculus and fractal geometry to provide a more complete understanding of the behavior of fractal functions. The power law, the exponential day law, and the generalized Mittag-Leffler law are the three most significant ones that have been proposed for this subject [7]. Research papers on Fractal fractional calculus have explored its applications in various fields such as finance, physics, and biology. A notable example is the paper "Fractal Fractional Calculus and Financial Markets" by [8]. In this paper, the authors demonstrate how FFC can be used to model the long-term memory behavior of financial time series. Another paper, "Fractal Fractional Calculus and Anomalous Diffusion in Complex Systems" by [9], shows how FFC can be used to describe anomalous diffusion processes in physical systems. In general, FFC provides a new way of looking at the derivatives of fractal functions and allows for the characterization of the complex behavior of these functions. Its applications in various fields demonstrate its potential for further exploration and use [10]. Since it has been shown that the power-law and exponential decay functions are more general than the kernel Mittag-Leffler function, the Riemann-Liouville and Caputo-Fabrizio fractional operators are particular instances of the Atangana-Baleanu fractional operators [11]. In Caputo-type circumstances, the existence of a local derivative of a power law, exponential function, or Mittag-Leffler function is crucial [12].

The early results are supported by a thorough qualitative investigation of the fractional-order HIV/AIDS model. Numerical simulations are carried out [13] to show the effects of changing the fractional order and to validate the theoretical conclusions using the methodologies offered for different fractional orders [14]. Nonlinear analysis was used to assess Ulam-Hyres' dependability [15]. The system of fractional differential equations is resolved using the Caputo and Atangana Baleanu fractional derivative operators. The fractional-order model has undergone qualitative analysis [16]. Numerical simulation is used to build the close-loop architecture and continuous glucose and insulin monitoring of the artificial pancreas. The created model provides the estimated values for the human glucose-insulin system's daily measurements [17]. Fractional derivatives exhibit large alterations and memory effects in contrast to conventional derivatives, which enable early disease identification and lower the risk of death [18]. Mathematical models can be used to investigate social behavior or the spread of infectious diseases. Numerous works on this topic and related topics have been applied to and researched in the social, medical, and political sciences [19]. Only a few mathematical research and investigations have been done on this topic, and the majority of them have concentrated on the phenomenon's statistical component [20]. It is possible to employ mathematical models to study social behavior or the spread of infectious illnesses. Several drinking-related mathematical models have been developed and investigated to lower the number of drinkers [21]. Adu [22] investigated the dynamics of the drinking pandemic using a nonlinear SHTR mathematical model. A mathematical model was created by Manthey et al. [23] to investigate the epidemiology model of ground drinking dynamics. Because there weren't enough reproductive persons to forecast if drinking patterns will endure on the campus, their data demonstrated that the strategy of enlisting new members had a significant influence on the reduction of ground alcohol issues. Sharma et al. [24] developed a two-stage (four compartments) method for the treatment of young individuals with serious drinking problems who have both admitted to their issue and have not. The stability of each equilibrium was also investigated.

COVID-19 fractional order models have gained significant attention in recent times, especially in the context of analyzing the spread of the disease. A fractional-order SIR model was proposed to study the spread of COVID-19. The model takes into account the time-varying parameters, which makes it more realistic compared to other models. The proposed model was used to analyze the data of some countries and the results showed that the fractional order SIR model can provide more accurate predictions than the traditional SIR model [25]. Another fractional-order SEIR model was proposed to study the transmission dynamics of COVID-19. The model takes into account the exposed and infected compartments, which makes it more comprehensive than the SIR model. The proposed model was used to analyze the data of some countries and the results showed that the fractional order SEIR model can provide more accurate predictions than the traditional SEIR model [26]. A fractional order SIR and SEIR models with saturating incidence rates are proposed to study the spread of COVID-19. The proposed models take into account the saturation in the transmission rate, which makes them more realistic compared to other models. The models were used to analyze the data of some countries and the results showed that the fractional order SIR and SEIR models with saturating incidence rates can provide more accurate predictions than the traditional SIR and SEIR models. Furthermore, the Authors of [27-31] research works have significantly contributed to the field of COVID-19 and pneumonia fractional order models analysis. His proposed models take into account various realistic factors and provide more accurate predictions compared to traditional models.

Because of their limitations at birth, working with nonsingular kernels is a difficult undertaking, as Refai and Baleanu discovered. In this brief study, we propose an extension of the fractional operator that permits an integrable singular kernel at the origin by involving the Mittag-Leffler kernel. New solutions to the associated differential equations were presented along with various modeling-related viewpoints [32]. By replacing this f'(t) with a more generic proportional derivative, Baleanu et al. [33] develop a new fractional operator. This novel operator can also be expressed as a linear combination of a Riemann Liouville integral and a Caputo derivative in some significant particular instances, or as a RiemanN Liouville integral of a proportionate derivative. For neural networks with ring or hub architectures, the stability area of a steady state has been extensively characterised, and the critical fractional order values for which Hopf bifurcations may occur have been discovered [34]. An example of fractional-order neural networks with mixed delays that exhibit periodic oscillation caused by delays in [35]. The dynamics of the model have changed, according to simulations. With the aid of fractional values and discoveries from multiple dimensions, the findings of the nonlinear system memory were also identified. Without imposing any more requirements, it provides a better technique for how you want to manage the sickness. The numerical results show how the dynamics in the different fractional orders behave [36,37]. Some application of modified Atangana-Baleanu [38], piecewise fractional analysis [39], intravenous drug model [40],piecewise constant for chemo-immunotherapy [41], SEIQR model [42] and HIV/AIDS with new fractional techniques in [43].

Section 2 provides the conception of the model as well as a few key aspects. The stability of the proposed model's equilibria is assessed in section 3 along with their identification. Some numerical simulations and comments are included in Section 4. The findings and discussions are covered in Section 5. Finally, we offer a summary of the paper's main findings.

2 Basic Definitions

This section has outlined a few preliminary steps that are essential for assessing the system.

2.1 Definition

Suppose the differential function $z(t)$, Let $\alpha \leq 0$ and $0 < \eta \leq 0$, Where η is fractal dimension and α is fractal order is given as COVID-19 model with a fractional operator that incorporates diabetes [44]

$$ {}_0^{FFP}D_t^{\alpha,\eta} z(t) = \frac{1}{\Gamma(1-\alpha)} \frac{d}{dt^{\eta}} \int_0^t z(\tau)(t-\tau)^{-\alpha} d\tau \tag{1} $$

Where

$$ \frac{dz(t)}{dt^{\eta}} = \lim_{t \to t_1} \frac{z(t) - z(t_1)}{t^{2-\eta} - {t_1}^{2-\eta}} \tag{2} $$

Given is an exponential kernel with a generalized fractional operator.

$$ {}_0^{FFE}D_t^{\alpha,\eta} z(t) = \frac{M(\alpha)}{1-\alpha} \frac{d}{dt^{\eta}} \int_0^t z(\tau) exp\big[-\frac{\alpha}{1-\alpha}(t-\tau)\big] d\tau \tag{3} $$

The generalized version of a Mittag Leffler kernel with a fractional operator is given as

$$ {}_0^{FFM}D_t^{\alpha,\eta} z(t) = \frac{AB(\alpha)}{1-\alpha} \frac{d}{dt^{\eta}} \int_0^t z(\tau) E_{\alpha}\big[-\frac{\alpha}{1-\alpha}(t-\tau)^{\alpha}\big] d\tau \tag{4} $$

*Remark.*Let f be continuous, if ${}_0^{FFE}D_t^{\alpha,\beta}$ exist [45,46], then for example

$$ \begin{aligned} {}_0^{FFE}D_t^{\alpha,\eta} g(t) &= \lim_{t \to t_1} \frac{G(t) - G(t_1)}{t - t_1} \frac{t - t_1}{t^{2-\eta} - t_1^{2-\eta}(2-\eta)} \\ &= G'(t) \frac{1}{t^{1-\eta}} \\ &= \frac{AB(\alpha)}{1-\alpha} \frac{d}{dt} \int_0^t g(\tau) E_{\alpha}[-\frac{\alpha}{1-\alpha}(t-\tau)^{\alpha}] \frac{d\tau}{t^{1-\eta}} \\ &= \frac{AB(\alpha)}{1-\alpha} \frac{d}{dt} \int_0^t g(\tau) E_{\alpha}[-\frac{\alpha}{1-\alpha}(t-\tau)^{\alpha}] d(\tau,t) \end{aligned} \tag{5} $$

Here $d(\tau,t) = \frac{d\tau}{t^{1-\eta}}$ is referred to as the fractal differential of variable τ and fractal representation $\frac{1}{t^{1-\eta}}$.

3 Fractional Order COVID-19 SEIR Model

We consider a novel model of COVID-19 with infectious force in latent period given in [47] having five compartments such as S(t), E(t), W(t), I(t), and R(t) respectively. We have followings non linear model with fractal fractional operator

$$\begin{aligned}
{}_0^{FFM}D_t^{\alpha,\eta}S(t) &= -\beta I(t)S(t)+\Lambda(1-m)+k_2W(t)-mS(t)-\mu S(t)\\
{}_0^{FFM}D_t^{\alpha,\eta}E(t) &= \beta I(t)S(t)-k_1E(t)-\varepsilon E(t)-\mu E(t)\\
{}_0^{FFM}D_t^{\alpha,\eta}W(t) &= k_1E(t)-\vartheta W(t)-k_2W(t)-\mu W(t)\\
{}_0^{FFM}D_t^{\alpha,\eta}I(t) &= \varepsilon E(t)-\vartheta I(t)-\gamma I(t)-\mu I(t)\\
{}_0^{FFM}D_t^{\alpha,\eta}R(t) &= \vartheta W(t)+\vartheta I(t)+m(\Lambda+S(t))-\mu R(t)
\end{aligned} \tag{6}$$

with $S(0)\geq 0$, $E(0)\geq 0$, $W(0)\geq 0$, $I(0)\geq 0$,$R(0)\geq 0$ are given initial states. The number of people that are COVID-19 virus susceptible but have no immunity is denoted by the symbol S(t). E(t) stands for the number of exposed people who haven't been quarantined. The number of exposed persons under quarantine is denoted by W(t). It indicates the number of infected people that show symptoms and are able to spread several retrieved people with positive medical test results and COVID-19 viral immunity is represented by R(t). Here m stands for the success percentage of vaccination in those at risk, which indicates the likelihood of developing immunity following vaccination, and β signifies the ratio of infected persons infecting susceptible ones. the government control rate is represented by k_1, ϑ represents the recovery rate, k_2 shows the autoimmune virus rate, Λ represents the rate of community growth, taking into account both foreigners and new babies, μ denotes the natural mortality, and γ shows the disease mortality. ε stands for the conversion rates from the exposed, non-quarantined population to the infected population.

3.1 Positiveness and Boundness of Model

Theorem 3.1

In straight-line conditions, the COVID-19 SEIR model suggested solution is distinct and constrained in R_+^5

Proof

We have got

$$\begin{aligned}
D_t^{\alpha,\eta}S(t) &= \Lambda(1-m)+k_2W(t)\geq 0\\
D_t^{\alpha,\eta}E(t) &= \beta I(t)S(t)\geq 0\\
D_t^{\alpha,\eta}W(t) &= k_1E(t)\geq 0\\
D_t^{\alpha,\eta}I(t) &= \varepsilon E(t)\geq 0\\
D_t^{\alpha,\eta}R(t) &= \vartheta W(t)+\vartheta I(t)+m(\Lambda+S(t))\geq 0
\end{aligned} \tag{7}$$

If $(S(0),E(0),W(0),I(0),R(0))\varepsilon R_+^5$, then the solution cannot escape from hyperplane. The domain R_+^5 is a positivity invariant set since the vector field on each hyperplane enclosing the non-negative orthant likewise points into it.

3.2 Global derivative effect on model

The Riemann-Stieltjes integral is the more widespread integral for which a specific example is the classical integral, as has long been known in the literature. The area under the curve of function $f(x)$ is how the geometric meaning of the traditional Riemann integral is expressed for instance if

$$F(x)=\int f(x)dx \tag{8}$$

The function $g(x)$ with respect to the function f has the following Riemann-Stieltjes integral:

$$F_g(x)=\int f(x)dg(x) \tag{9}$$

No differential calculus is connected to the more general integral calculus created by the generalized integral operator. Recently, it was proposed and demonstrated that the Riemann-Stieltjes integral is related to the idea of global differentiation. Given is a function's global derivative about another function, g(x):

$$D_g f(x) = \lim_{h\to 0} \frac{f(x+h)-f(x)}{g(x+h)-g(x)} \tag{10}$$

Consequently, we have if function is differentiable

$$D_g f(x) = \frac{f'(x)}{g'(x)} \tag{11}$$

Giving that $g'(x) \neq 0, \forall x \in \mathbb{D}'_g$

In this part, we'll utilize this idea to examine its potential impact on the exogenous growth model. We will use the global derivative in place of the conventional derivative to achieve this.

$$\begin{aligned}
D_g S(t) &= -\beta I(t)S(t) + \Lambda(1-m) + k_2 W(t) - mS(t) - \mu S(t) \\
D_g E(t) &= \beta I(t)S(t) - k_1 E(t) - \varepsilon E(t) - \mu E(t) \\
D_g W(t) &= k_1 E(t) - \vartheta W(t) - k_2 W(t) - \mu W(t) \\
D_g I(t) &= \varepsilon E(t) - \vartheta I(t) - \gamma I(t) - \mu I(t) \\
D_g R(t) &= \vartheta W(t) + \vartheta I(t) + m(\Lambda + S(t)) - \mu R(t)
\end{aligned} \tag{12}$$

For further solution, consider g is differentiable, then

$$\begin{aligned}
S' &= g'[-\beta I(t)S(t) + \Lambda(1-m) + k_2 W(t) - mS(t) - \mu S(t)] = J_1(t,\xi) \\
E' &= g'[\beta I(t)S(t) - k_1 E(t) - \varepsilon E(t) - \mu E(t)] = J_2(t,\xi) \\
W' &= g'[k_1 E(t) - \vartheta W(t) - k_2 W(t) - \mu W(t)] = J_3(t,\xi) \\
I' &= g'[\varepsilon E(t) - \vartheta I(t) - \gamma I(t) - \mu I(t)] = J_4(t,\xi) \\
R' &= g'[\vartheta W(t) + \vartheta I(t) + m(\Lambda + S(t)) - \mu R(t)] = J_5(t,\xi)
\end{aligned} \tag{13}$$

Where

$$\xi = S, E, W, I, R \tag{14}$$

For $g(t) = t^{\alpha}, \alpha \in \mathbb{R}$, we have particular form under the condition

$$\| g' \|_{\infty} = \sup_{t \in D'_g} < N \tag{15}$$

For unique solution of equation (16), need to verify these two conditions

–$| J(t,S,E,W,I,R) < \kappa(1+|S|^2) |$
–$\forall S_1, S_2$ we have $\|J(t,S_1,E,W,I,R) - J(t,S_2,E,W,I,R)\| < \kappa \|S_1 - S_2\|_{\infty}^2$

Initially,

$$\begin{aligned}
|J_1(t,S,E,W,I,R)|^2 &= |g'[-\beta I(t)S(t) + \Lambda(1-m) + k_2 W(t) - mS(t) - \mu S(t)]|^2 \\
&\leq 2|g'|^2[|(\Lambda(1-m) + k_2 W(t))|^2 + |(-\beta I(t) - m - \mu)S(t)|^2] \\
&\leq 2|g'|^2(|\Lambda(1-m) + k_2 W(t)|^2 + (-\beta I(t) - m - \mu)^2 |S(t)|^2) \\
&\leq 2|g'|^2 \Lambda(1-m) + k_2 W(t)|^2 (1 + \frac{(-\beta I(t) - m - \mu)^2 |S(t)|^2}{|\Lambda(1-m) + k_2 W(t)|^2}) \\
&< \kappa_1(1+|S|^2)
\end{aligned} \tag{16}$$

Under the condition

$$\frac{(-\beta I(t) - m - \mu)^2 |S(t)|^2}{|\Lambda(1-m) + k_2 W(t)|^2} < 1 \tag{17}$$

Where

$$\kappa_1 = 2|g'|^2\Lambda(1-m) + k_2|W(t)|^2 \tag{18}$$

$$\begin{aligned} |J_2(t,S,E,W,I,R)|^2 &= |g'[\beta I(t)S(t) - k_1E(t) - \varepsilon E(t) - \mu E(t)]|^2 \\ &\leq |g'[\beta I(t)S(t) + (-k_1 - \varepsilon - \mu)E(t)]|^2 \\ &\leq 2|g'|^2[|\beta I(t)S(t)|^2 + (-k_1 - \varepsilon - \mu)|E(t)|^2] \\ &\leq 2|g'|^2|\beta I(t)S(t)|^2(1 + \frac{(-k_1 - \varepsilon - \mu)|E(t)|^2)}{|\beta I(t)S(t)|^2} \\ &< \kappa_2(1 + |E|^2) \end{aligned} \tag{19}$$

Under the condition

$$\frac{(-k_1 - \varepsilon - \mu)|E(t)|^2)}{|\beta I(t)S(t)|^2} < 1 \tag{20}$$

Where

$$\kappa_2 = 2|g'|^2|\beta I(t)S(t)|^2 \tag{21}$$

$$\begin{aligned} |J_3(t,S,E,W,I,R)|^2 &= |g'[k_1E(t) - \vartheta W(t) - k_2W(t) - \mu W(t)]|^2 \\ &\leq 2|g'|^2(|k_1E(t)|^2 + (-\vartheta - k_2 - \mu)^2|W(t)|^2) \\ &\leq 2|g'|^2|k_1E(t)|^2(1 + \frac{(-\vartheta - k_2 - \mu)^2|W(t)|^2)}{|k_1E(t)|^2} \\ &< \kappa_3(1 + |W|^2) \end{aligned} \tag{22}$$

Under the condition

$$\frac{(-\vartheta - k_2 - \mu)^2|W(t)|^2)}{|k_1E(t)|^2} < 1 \tag{23}$$

Where

$$\kappa_3 = 2|g'|^2|k_1E(t)|^2 \tag{24}$$

$$\begin{aligned} |J_4(t,S,E,W,I,R)|^2 &= |g'[\varepsilon E(t) - \vartheta I(t) - \gamma I(t) - \mu I(t)]|^2 \\ &\leq 2|g'|^2[|\varepsilon E(t)|^2 + (-\vartheta - \gamma - \mu)|I(t)|^2] \\ &\leq 2|g'|^2|\varepsilon E(t)|^2(1 + \frac{(-\vartheta - \gamma - \mu)|I(t)|^2)}{|\varepsilon E(t)|^2} \\ &< \kappa_4(1 + |I|^2) \end{aligned} \tag{25}$$

Under the condition

$$\frac{(-\vartheta - \gamma - \mu)|I(t)|^2)}{|\varepsilon E(t)|^2} < 1 \tag{26}$$

Where

$$\kappa_4 = 2|g'|^2|\varepsilon E(t)|^2 \tag{27}$$

$$\begin{aligned}|J_5(t,S,E,W,I,R)|^2 &= |g'[\vartheta W(t)+\vartheta I(t)+m(\Lambda+S(t))-\mu R(t)]|^2 \\ &\leq 2|g'|^2[|\vartheta W(t)+\vartheta I(t)+m(\Lambda+S(t))|^2-|\mu R(t)|^2] \\ &\leq 2|g'|^2[\vartheta|W(t)|^2+\vartheta|I(t)|^2+|m(\Lambda+S(t))|^2-\mu|R(t)|^2] \\ &\leq 2|g'|^2\vartheta|W(t)|^2+\vartheta|I(t)|^2+|m(\Lambda+S(t))|^2 \\ &\quad (1-\frac{\mu|R(t)|^2}{\vartheta|W(t)|^2+\vartheta|I(t)|^2+|m(\Lambda+S(t))|^2}) \\ &< \kappa_5(1+|R|^2)\end{aligned} \tag{28}$$

Under the condition

$$\frac{\mu|R(t)|^2}{\vartheta|W(t)|^2+\vartheta|I(t)|^2+|m(\Lambda+S(t))|^2} > 1 \tag{29}$$

Where

$$\kappa_5 = 2|g'|^2\vartheta|W(t)|^2+\vartheta|I(t)|^2+|m(\Lambda+S(t))|^2 \tag{30}$$

Hence it is proved that it is defined for linear growth condition Further, we validate the Lipschitz condition. If

$$\begin{aligned}|J_1(t,S_1,E,W,I,R)-J_1(t,S_2,E,W,I,R)|^2 &= |(-\beta I(t)-m-\mu)|^2|(S_1-S_2)|^2 \\ &\leq 22\beta^2|I(t)|^2+2(m+\mu)^2|(S_1-S_2)|^2 \\ &\leq 4\beta^2\sup_{t\in D_I}|I(t)|^2+4(m+\mu)^2\sup_{t\in D_S}|(S_1-S_2)|^2 \\ &\leq 4\beta^2\|I(t)\|_\infty^2+4(m+\mu)^2\|(S_1-S_2)\|_\infty^2 \\ &\leq \bar{\kappa_1}\|S_1-S_2\|_\infty^2\end{aligned} \tag{31}$$

Where

$$\bar{\kappa_1} = 4\beta^2\|I(t)\|_\infty^2+4(m+\mu)^2 \tag{32}$$

$$\begin{aligned}|J_2(t,S,E_1,W,I,R)-J_2(t,S,E_2,W,I,R)|^2 &= (-k_1-\varepsilon-\mu)|^2|(E_1-E_2)|^2 \\ &\leq |(-k_1-\varepsilon-\mu)|^2\sup_{t\in D_E}|(E_1-E_2)|^2 \\ &\leq |(-k_1-\varepsilon-\mu)|^2\|(E_1-E_2)\|_\infty^2 \\ &\leq \bar{\kappa_2}\|E_1-E_2\|_\infty^2\end{aligned} \tag{33}$$

Where

$$\bar{\kappa_2} = (-k_1-\varepsilon-\mu)|^2 \tag{34}$$

$$\begin{aligned}|J_3(t,S,E,W_1,I,R)-J_3(t,S,E,W_2,I,R)|^2 &= (-\vartheta-k_2-\mu)^2|(W_1-W_2)|^2 \\ &\leq (-\vartheta-k_2-\mu)^2\sup_{t\in D_W}|(W_1-W_2)|^2 \\ &\leq (-\vartheta-k_2-\mu)^2\|(W_1-W_2)\|_\infty^2 \\ &\leq \bar{\kappa_3}\|W_1-W_2\|_\infty^2\end{aligned} \tag{35}$$

Where

$$\bar{\kappa_3} = (-\vartheta - k_2 - \mu)^2 \tag{36}$$

$$\begin{aligned} |J_4(t,S,E,W,I_1,R) - J_4(t,S,E,W,I_2,R)|^2 &= (-\vartheta-\gamma-\mu)^2|(I_1-I_2)|^2 \\ &\leq (-\vartheta-\gamma-\mu)^2 \sup_{t\in D_I}|(I_1-I_2)|^2 \\ &\leq (-\vartheta-\gamma-\mu)^2\|(I_1-I_2)\|_\infty^2 \\ &\leq \bar{\kappa_4}\|I_1-I_2\|_\infty^2 \end{aligned} \tag{37}$$

Where

$$\bar{\kappa_4} = (-\vartheta-\gamma-\mu)^2 \tag{38}$$

$$\begin{aligned} |J_5(t,S,E,W,I,R_1) - J_5(t,S,E,W,I,R_2)|^2 &= \mu^2|(R_1-R_2)|^2 \\ &\leq \mu^2 \sup_{t\in D_I}|(R_1-R_2)|^2 \\ &\leq \mu^2\|(R_1-R_2)\|_\infty^2 \\ &\leq \bar{\kappa_5}\|R_1-R_2\|_\infty^2 \end{aligned} \tag{39}$$

Where

$$\bar{\kappa_5} = \mu^2 \tag{40}$$

3.3 Reproduction Number and Sensitivity Analysis of system

Several secondary cases generated by a solitary diseased person in a susceptible group during the illness are the fundamental reproduction number. Using the approach of the next-generation operator, we calculate the reproduction number.

$$R_0 = \frac{\beta\varepsilon S_0}{(\mu+k_1+\varepsilon)(\mu+\vartheta+\gamma)} \tag{41}$$

For sensitivity analysis by using reproductive number, we have

$$\frac{\partial R_0}{\partial \beta} = \frac{\varepsilon S_0}{(\mu+k_1+\varepsilon)(\mu+\vartheta+\gamma)} > 0 \tag{42}$$

$$\frac{\partial R_0}{\partial \varepsilon} = 0 \tag{43}$$

$$\frac{\partial R_0}{\partial \mu} = -\frac{(\beta\varepsilon S_0)(2\mu+\varepsilon+\vartheta+\gamma+k_1)}{(\mu+k_1+\varepsilon)^2(\mu+\vartheta+\gamma)^2} < 0 \tag{44}$$

$$\frac{\partial R_0}{\partial k_1} = -\frac{\beta\varepsilon S_0}{(\mu+k_1+\varepsilon)^2(\mu+\vartheta+\gamma)} < 0 \tag{45}$$

$$\frac{\partial R_0}{\partial \vartheta} = -\frac{(\beta\varepsilon S_0)}{(\mu+k_1+\varepsilon)(\mu+\vartheta+\gamma)^2} < 0 \tag{46}$$

$$\frac{\partial R_0}{\partial \gamma} = -\frac{(\beta\varepsilon S_0)}{(\mu+k_1+\varepsilon)(\mu+\vartheta+\gamma)^2} < 0 \tag{47}$$

Here, we observe that, β is expanding while μ, k_1, ϑ and γ are contracting and $\varepsilon = 0$.

3.4 Equilibrium Points Analysis

The two distinct kinds of equilibrium points are disease-present equilibrium points and complaint-free equilibrium points. To discover them, the right-hand sides of the system's equations are set to zero.

Theorem 3.2

If $R_0 > 1$, then the proposed model has $P_0(0,0,S_0,0)$ and virus existing steady states $P^*(E^*,I^*,S^*,W^*)$. Otherwise, there is only virus free steady state $P_0(0,0,S_0,0)$ with $S_0 = \frac{\Lambda(1-m)}{m+\mu}$. So,

$$\begin{aligned} S^* &= \frac{\omega_1\omega_2}{\beta\varepsilon} \\ E^* &= \frac{\omega_3\omega_1\omega_2\theta(1-R_0)}{\beta\varepsilon(k_1k_2-\omega_1\omega_3)} \\ W^* &= \frac{k_1}{\omega_3}E^* \\ I^* &= \frac{\varepsilon}{\omega_2}E^* \end{aligned} \tag{48}$$

Where

$$\begin{aligned} \omega_1 &= \mu + k_1 + \varepsilon \\ \omega_2 &= \mu + \vartheta + \gamma \\ \omega_3 &= \mu + \vartheta + k_2 \\ \theta &= m + \mu \end{aligned} \tag{49}$$

Theorem 3.2

Let $\Pi : [0,T] \times B \to \mathbb{R}$ be a continuous function. The system having at least one solution is conditioned in [48].

Proof:

First of all considering the equation (**??**) is completely continuous which describe with operator $\aleph$. Since Λ and $\aleph$ are continuous operators.
Suppose that $H = \{\Pi \in B : \|\Pi\| \leq R, R > 0\}$. For some $\Pi \in B$, we have

$$|\aleph(\Pi)(t)| = \max_{t\in[0,T]} |\Pi(0) + \frac{\alpha t^{\alpha-1}(1-\alpha)}{AB(\alpha)}\Lambda(t,\Pi(t)) + \frac{\alpha\eta}{AB(\alpha)\Gamma(\alpha)}\int_0^t t^{\alpha-1}(t-\tau)^{\alpha-1}\Lambda(t,\Pi(t))d\tau|. \tag{50}$$

$$\leq \Pi(0) + \frac{\alpha t^{\alpha-1}(1-\alpha)}{AB(\alpha)}(C_\Lambda\|\Pi\| + M_\Lambda) + \max_{t\in[0,T]}\frac{\alpha\eta}{AB(\alpha)\Gamma(\alpha)}\int_0^t t^{\alpha-1}(t-\tau)^{\alpha-1}\Lambda(t,\Pi(t))d\tau|. \tag{51}$$

$$\leq \Pi(0) + \frac{\alpha t^{\alpha-1}(1-\alpha)}{AB(\alpha)}(C_\Lambda\|\Pi\| + M_\Lambda) + \frac{\alpha\eta}{AB(\alpha)\Gamma(\alpha)}(C_\Lambda\|\Pi\| + M_\Lambda)T^{\alpha+\eta-1}H(\alpha,\eta). \tag{52}$$

$$\leq R. \tag{53}$$

Therefore, we get

$$\begin{aligned} |\aleph(\Pi)(t_2) - \aleph(\Pi)(t_1)| = \max_{t\in[0,T]} |&\frac{\alpha t^{\alpha-1}(1-\alpha)}{AB(\alpha)}\Lambda(t_2,\Pi(t_2)) + \frac{\alpha\eta}{AB(\alpha)\Gamma(\alpha)}\int_0^t t^{\alpha-1}(t-\tau)^{\alpha-1}\Lambda(t_2,\Pi(t_2))d\tau \\ &- \frac{\alpha t^{\alpha-1}(1-\alpha)}{AB(\alpha)}\Lambda(t_1,\Pi(t_1)) - \frac{\alpha\eta}{AB(\alpha)\Gamma(\alpha)}\int_0^t t^{\alpha-1}(t-\tau)^{\alpha-1}\Lambda(t_1,\Pi(t_1))d\tau|. \end{aligned} \tag{54}$$

$$\begin{aligned}&\leq \frac{\alpha t^{\alpha-1}(1-\alpha)}{AB(\alpha)}(C_\Lambda\|\Pi\|+M_\Lambda)+\frac{\alpha\eta}{AB(\alpha)\Gamma(\alpha)}(C_\Lambda\|\Pi\|+M_\Lambda)T^{\alpha+\eta-1}H(\alpha,\eta)\\&-\frac{\alpha t^{\alpha-1}(1-\alpha)}{AB(\alpha)}(C_\Lambda\|\Pi\|+M_\Lambda)-\frac{\alpha\eta}{AB(\alpha)\Gamma(\alpha)}(C_\Lambda\|\Pi\|+M_\Lambda)T^{\alpha+\eta-1}H(\alpha,\eta).\end{aligned} \tag{55}$$

When $t_1 \to t_2$ then $|\aleph(\Pi)(t_2)-\aleph(\Pi)(t_1)| \to 0|$. $\|\aleph(\Pi)(t_2)-\aleph(\Pi)(t_1)\| \to 0$ as $t_1 \to t_2$. Thus, $\aleph$ is equicontinuous. Then, by Schauders fixed point result its hold the condition.

3.5 Local stability Analysis

It is commonly known that whether a disease will disappear or remain in the population depends on the fundamental reproductive number. Recall that the sickness will eventually disappear when $R_0 < 1$. (no epidemic). In the meanwhile, the sickness will spread rapidly if $R_0 > 1$. Additionally, the value of R_0 shows how infectious the illness is. The stability of the steady states connected to the fractional model will then be examined. Two theorems are stated for this goal [49].

Theorem 3.4

If $R_0 < 1$ then the virus-free steady state is locally stable

Proof

The linearized system according to $P_0(0,0,S_0,0)$ is given by

$$F(P_0)=\begin{bmatrix}-T_1 & \beta S_0 & 0 & 0\\ \varepsilon & -T_2 & 0 & 0\\ 0 & -\beta S_0 & -\theta & k_2\\ k_1 & 0 & 0 & -T_3\end{bmatrix}$$

The characteristic equation of $F(P_0)$ is given as

$$f(\lambda)=(\lambda+T_1)(\lambda+T_2)(\lambda+T_3)(\lambda+\theta)-\beta S_0\varepsilon(\lambda+\theta)(\lambda+T_3)=0 \tag{56}$$

Which leads to

$$(\lambda+T_1)(\lambda+T_2)-\beta S_0\varepsilon=0 \tag{57}$$

It can appear that all roots have true negative components. Therefore, $P_0(0,0,S_0,0)$ of the system is locally asymptotically stable.

Theorem 3.5

If $R_0 > 1$ then the virus existing steady state is locally stable

Proof

The Jacobian matrix of the given model according to $P^*(S^*,E^*,W^*,I^*)$ is given by

$$F(P^*)=\begin{bmatrix}-T_1 & \beta S^* & \beta I^* & 0\\ \varepsilon & -T_2 & 0 & 0\\ 0 & -\beta S^* & -\beta I^*-\theta & k_2\\ k_1 & 0 & 0 & -T_3\end{bmatrix}$$

The characteristic equation of $F(P^*)$ is given as

$$f(\lambda)=(\lambda+T_1)(\lambda+T_2)(\lambda+T_3)(\lambda+-\beta I^*+\theta)-\beta S^*\varepsilon(\lambda+\theta)(\lambda+T_3)-k_1k_2\beta I^*(\lambda+T_2)=0 \tag{58}$$

It can appear that all roots have true negative components. As a result, the model's $P*(S^*,E^*,W^*,I^*)$ is locally asymptotically stable.

3.6 Global Stablity Analysis

The Lyapunov method and LaSalle's invariance principle are used to illustrate the global stability analysis, which identifies the prerequisites for disease eradication.

3.6.1 Lyapunov's First Derivative

Where $V < 0$, the endemic equilibrium for the endemic Lyapunov function is (S, E, W, I, R).

Theorem 3.6

When the reproductive number $R_0 > 1$, the virus existing steady state of this model is globally asymptotically stable.

Proof

Considering Lyapunov function, we have

$$V = K_1(S - S^* - S^* ln\frac{S^*}{S}) + K_2(E - E^* - E^* ln\frac{E^*}{E}) + K_3(W - W^* - W^* ln\frac{W^*}{W})$$
$$+ K_4(I^* - I^* - I^* ln\frac{I^*}{I^*}) + K_5(R - R^* - R^* ln\frac{R^*}{R})$$

Where, $K_i, i = 1,2,3,4,5$ are all positive constants that can be chosen later. By substituting the above equation into the system we get

$$\begin{aligned} {}_0^{FFM}D_t^{\eta}V \leq\ & K_1(1 - \frac{S^*}{S})\,{}_0^{FFM}D_t^{\eta}S + K_2(1 - \frac{E^*}{E})\,{}_0^{FFM}D_t^{\eta}E + K_3(1 - \frac{W^*}{W}) \\ & {}_0^{FFM}D_t^{\eta}W + K_4(1 - \frac{I^*}{I})\,{}_0^{FFM}D_t^{\eta}I + K_5(1 - \frac{R^*}{R})\,{}_0^{FFM}D_t^{\eta}R \end{aligned} \tag{59}$$

$$\begin{aligned} {}_0^{FFM}D_t^{\eta}V \leq\ & K_1(1 - \frac{S^*}{S})(-\beta I(t)S(t) + \Lambda(1-m) + k_2W(t) - mS(t) - \mu S(t)) + K_2(1 - \frac{E^*}{E}) \\ & (\beta I(t)S(t) - k_1E(t) - \varepsilon E(t) - \mu E(t)) + K_3(1 - \frac{W^*}{W})(k_1E(t) - \vartheta W(t) - k_2W(t) \\ & - \mu W(t)) + K_4(1 - \frac{I^*}{I})(\varepsilon E(t) - \vartheta I(t) - \gamma I(t) - \mu I(t))I + K_5(1 - \frac{R^*}{R}) \\ & (\vartheta W(t) + \vartheta I(t) + m(\Lambda + S(t)) - \mu R(t)) \end{aligned}$$

After the computations and by setting $K_1 = K_2 = K_3 = K_4 = K_5 = 1$, we obtain

$$\begin{aligned} {}_0^{FFM}D_t^{\eta}V \leq\ & (\frac{S - S^*}{S})(-\beta(I - I^*)(S - S^*) + \Lambda(1-m) + k_2(W - W^*) - m(S - S^*) - \mu(S - S^*)) \\ & + (\frac{E - E^*}{E})(\beta(I - I^*)(S - S^*) - k_1(E - E^*) - \varepsilon(E - E^*) - \mu(E - E^*)) + (\frac{W - W^*}{W}) \\ & (k_1(E - E^*) - \vartheta(W - W^*) - k_2(W - W^*) - \mu(W - W^*)) + (\frac{I - I^*}{I})(\varepsilon(E - E^*) \\ & - \vartheta(I - I^*) - \gamma(I - I^*) - \mu(I - I^*)) + (\frac{R - R^*}{R})(\vartheta(W - W^*) + \vartheta(I - I^*) \\ & + m(\Lambda + (S - S^*)) - \mu(R - R^*)) \\ & \leq 0 \end{aligned}$$

where ${}_0^{FFM}D_t^{\eta}V \leq 0$ for $R_0 > 1$, and ${}_0^{FFM}D_t^{\eta}V = 0$ only if $S = S^*, E = E^*, W = W^*, I = I^*$. Therefore, it is concluded that the given system is globally asymptotically stable.

3.6.2 Second derivative of Lyapunov

$$
\begin{aligned}
{}_0^{FFM}\dot{D}_t^{\eta}V &= ({}_0^{FFM}D_t^{\eta}\frac{S}{S})^2S^* + ({}_0^{FFM}D_t^{\eta}\frac{E}{E})^2E^* + ({}_0^{FFM}D_t^{\eta}\frac{W}{W})^2W^* + ({}_0^{FFM}D_t^{\eta}\frac{I}{I})^2I^* + ({}_0^{FFM}D_t^{\eta}\frac{R}{R})^2R^* \\
&+ (1-\frac{S^*}{S})\,{}_0^{FFM}\dot{D}_t^{\eta}S + (1-\frac{E^*}{E})\,{}_0^{FFM}\dot{D}_t^{\eta}E + (1-\frac{W^*}{W})\,{}_0^{FFM}\dot{D}_t^{\eta}W + (1-\frac{I^*}{I})\,{}_0^{FFM}\dot{D}_t^{\eta}I + (1-\frac{R^*}{R})\,{}_0^{FFM}\dot{D}_t^{\eta}R
\end{aligned}
$$

Here

$$
\begin{aligned}
{}_0^{FFM}\dot{D}_t^{\eta}S(t) &= -\beta I(t)\,{}_0^{FFM}D_t^{\eta}S(t) - m_0^{FFM}D_t^{\eta}S(t) - \mu_0^{FFM}D_t^{\eta}S(t) \\
{}_0^{FFM}\dot{D}_t^{\eta}E(t) &= k_1\,{}_0^{FFM}D_t^{\eta}E(t) - \varepsilon_0^{FFM}D_t^{\eta}E(t) - \mu_0^{FFM}D_t^{\eta}E(t) \\
{}_0^{FFM}\dot{D}_t^{\eta}W(t) &= \vartheta_0^{FFM}D_t^{\eta}W(t) - k_2\,{}_0^{FFM}D_t^{\eta}W(t) - \mu_0^{FFM}D_t^{\eta}W(t) \\
{}_0^{FFM}\dot{D}_t^{\eta}I(t) &= \vartheta_0^{FFM}D_t^{\eta}I(T) - \gamma_0^{FFM}D_t^{\eta}I(t) - \mu_0^{FFM}D_t^{\eta}I(t) \\
{}_0^{FFM}\dot{D}_t^{\eta}R(t) &= -\mu_0^{FFM}D_t^{\eta}R(t)
\end{aligned}
\tag{60}
$$

Then

$$
\begin{aligned}
{}_0^{FFM}\dot{D}_t^{\eta}V &= ({}_0^{FFM}D_t^{\eta}\frac{S}{S})^2S^* + ({}_0^{FFM}D_t^{\eta}\frac{E}{E})^2E^* + ({}_0^{FFM}D_t^{\eta}\frac{W}{W})^2W^* + ({}_0^{FFM}D_t^{\eta}\frac{I}{I})^2I^* + ({}_0^{FFM}D_t^{\eta}\frac{R}{R})^2R^* \\
&+ (1-\frac{S^*}{S})(-\beta I(t)\,{}_0^{FFM}D_t^{\eta}S - m_0^{FFM}D_t^{\eta}S - \mu_0^{FFM}D_t^{\eta}S) + (1-\frac{E^*}{E})(k_1\,{}_0^{FFM}D_t^{\eta}E) - \varepsilon_0^{FFM}D_t^{\eta}E \\
&- \mu_0^{FFM}D_t^{\eta}E) + (1-\frac{W^*}{W})(\vartheta_0^{FFM}D_t^{\eta}W - k_2\,{}_0^{FFM}D_t^{\eta}W - \mu_0^{FFM}D_t^{\eta}W) + (1-\frac{I^*}{I})(\vartheta_0^{FFM}D_t^{\eta}I \\
&- \gamma_0^{FFM}D_t^{\eta}I - \mu_0^{FFM}D_t^{\eta}I) + (1-\frac{R^*}{R})(-\mu_0^{FFM}D_t^{\eta}R)
\end{aligned}
$$

Now let us consider that

$$
\dot{\Lambda}(S,E,W,I,R) = ({}_0^{FFM}D_t^{\eta}\frac{S}{S})^2S^* + ({}_0^{FFM}D_t^{\eta}\frac{E}{E})^2E^* + ({}_0^{FFM}D_t^{\eta}\frac{W}{W})^2W^* + ({}_0^{FFM}D_t^{\eta}\frac{I}{I})^2I^* + ({}_0^{FFM}D_t^{\eta}\frac{R}{R})^2R^*
$$

Then

$$
\begin{aligned}
{}_0^{FFM}\dot{D}_t^{\eta}V &= \dot{\Lambda}(S,E,W,I,R) + (1-\frac{S^*}{S})(-\beta I(t)\,{}_0^{FFM}D_t^{\eta}S - m_0^{FFM}D_t^{\eta}S - \mu_0^{FFM}D_t^{\eta}S) + (1-\frac{E^*}{E}) \\
&(k_1\,{}_0^{FFM}D_t^{\eta}E - \varepsilon_0^{FFM}D_t^{\eta}E - \mu_0^{FFM}D_t^{\eta}E) + (1-\frac{W^*}{W})(\vartheta_0^{FFM}D_t^{\eta}W - k_2\,{}_0^{FFM}D_t^{\eta}W \\
&- \mu_0^{FFM}D_t^{\eta}W) + (1-\frac{I^*}{I})(\vartheta_0^{FFM}D_t^{\eta}I - \gamma_0^{FFM}D_t^{\eta}I - \mu_0^{FFM}D_t^{\eta}I) + (1-\frac{R^*}{R})(-\mu_0^{FFM}D_t^{\eta}R)
\end{aligned}
$$

After replacing the values of the first derivatives we get
Which can be written as

$$
{}_0^{FFM}\dot{D}_t^{\eta}V = \wp_1 + \wp_2 \tag{61}
$$

$\wp_1$: Contain all positive values
$\wp_2$: Contain all negative values
It can be seen that

–If $\wp_1 > \wp_2$ then ${}_0^{FFM}\dot{D}_t^{\eta}V > 0$
–If $\wp_1 < \wp_2$ then ${}_0^{FFM}\dot{D}_t^{\eta}V < 0$
–If If $\wp_1 = \wp_2$ then ${}_0^{FFM}\dot{D}_t^{\eta}V = 0$

4 Computational Analysis with Fractal Fractional Operator

In this part, the suggested mathematical COVID-19 SEIR model is applied to the new differential and integral operators. Here, the operator with the Mittag-Leffler Kernel [50] will take the place of the conventional differential operator. The version with flexible order will also be used.

Since (7) we get

$$ {}_0^{FFM}D_t^{\alpha,\eta}S(t) = S_1(t,\xi) \tag{62}$$

$$ {}_0^{FFM}D_t^{\alpha,\eta}E(t) = E_1(t,\xi) \tag{63}$$

$$ {}_0^{FFM}D_t^{\alpha,\eta}W(t) = W_1(t,\xi) \tag{64}$$

$$ {}_0^{FFM}D_t^{\alpha,\eta}I(t) = I_1(t,\xi) \tag{65}$$

$$ {}_0^{FFM}D_t^{\alpha,\eta}R(t) = R_1(t,\xi) \tag{66}$$

By using Mittag-Leffler kernel we get,

$$S(t_{\delta+1}) = S_0 + \frac{1-\alpha}{AB(\alpha)}t_\delta^{1-\beta}S_1(t_\delta,S(t_\delta),E(t_\delta),W(t_\delta),I(t_\delta),R(t_\delta))$$
$$+\hbar\sum_{\mu=2}^{\delta}\int_{t_\mu}^{t_{\mu+1}} S_1(\tau,\xi)\tau^{1-\eta}(t_{\delta+1}-\tau)^{\alpha-1}d\tau$$

$$E(t_{\delta+1}) = E_0 + \frac{1-\alpha}{AB(\alpha)}t_\delta^{1-\beta}E_1(t_\delta,S(t_\delta),E(t_\delta),W(t_\delta),I(t_\delta),R(t_\delta))$$
$$+\hbar\sum_{\mu=2}^{\delta}\int_{t_\mu}^{t_{\mu+1}} E_1(\tau,\xi)\tau^{1-\eta}(t_{\delta+1}-\tau)^{\alpha-1}d\tau$$

$$W(t_{\delta+1}) = W_0 + \frac{1-\alpha}{AB(\alpha)}t_\delta^{1-\beta}W_1(t_\delta,S(t_\delta),E(t_\delta),W(t_\delta),I(t_\delta),R(t_\delta))$$
$$+\hbar\sum_{\mu=2}^{\delta}\int_{t_\mu}^{t_{\mu+1}} W_1(\tau,\xi)\tau^{1-\eta}(t_{\delta+1}-\tau)^{\alpha-1}d\tau$$

$$I(t_{\delta+1}) = I_0 + \frac{1-\alpha}{AB(\alpha)}t_\delta^{1-\beta}I_1(t_\delta,S(t_\delta),E(t_\delta),W(t_\delta),I(t_\delta),R(t_\delta))$$
$$+\hbar\sum_{\mu=2}^{\delta}\int_{t_{mu}}^{t_{\mu+1}} I_1(\tau,\xi)\tau^{1-\eta}(t_{\delta+1}-\tau)^{\alpha-1}d\tau$$

$$R(t_{\delta+1}) = R_0 + \frac{1-\alpha}{AB(\alpha)}t_\delta^{1-\beta}R_1(t_\delta,S(t_\delta),E(t_\delta),W(t_\delta),I(t_\delta),R(t_\delta))$$
$$+\hbar\sum_{\mu=2}^{\delta}\int_{t_\mu}^{t_{\mu+1}} R_1(\tau,\xi)\tau^{1-\eta}(t_{\delta+1}-\tau)^{\alpha-1}d\tau$$

Where $\xi = S,E,W,I,R$ and $\hbar = \frac{\alpha}{AB(\alpha)\Gamma(\alpha)}$, we get,

$$S^{\delta+1} = \frac{1-\alpha}{AB(\alpha)}t_\delta^{1-\eta}S_1(t_\delta,S^\delta,E^\delta,W^\delta,I^\delta,R^\delta) + \frac{\alpha(\Delta t)^\mu}{AB(\alpha)\Gamma(\alpha+1)} \tag{67}$$
$$\sum_{\mu=2}^{\delta} t_{\mu-2}^{1-\eta}S_1(\Theta)\times\Psi + \frac{\alpha(\Delta t)^\alpha}{AB(\alpha)\Gamma(\alpha+2)}$$
$$\sum_{\mu=2}^{\delta}\left[t_{\mu-1}^{1-\eta}S_1(\upsilon) - t_{\mu-2}^{1-\eta}S_1(\theta)\right]\times\Phi$$
$$+\frac{\alpha(\Delta t)^\alpha}{2AB(\alpha)\Gamma(\alpha+3)}\sum_{\mu=2}^{\delta}[t_\mu^{1-\eta}S_1(t_\mu,S^\mu,E^\mu,W^\mu,I^\mu,R^\mu) - 2t_{\mu-1}^{1-\eta}S_1(\upsilon)$$
$$- t_{\mu-2}^{1-\eta}S_1(\Theta)]\times\zeta$$

$$E^{\delta+1}=\frac{1-\alpha}{AB(\alpha)}t_{\delta}^{1-\eta}E_1(t_\delta,S^\delta,E^\delta,W^\delta,I^\delta,R^\delta)+\frac{\alpha(\Delta t)^{\mu}}{AB(\alpha)\Gamma(\alpha+1)} \tag{68}$$
$$\sum_{\mu=2}^{\delta}t_{\mu-2}^{1-\eta}E_1(\Theta)\times\Psi+\frac{\alpha(\Delta t)^{\alpha}}{AB(\alpha)\Gamma(\alpha+2)}$$
$$\sum_{\mu=2}^{\delta}\left[t_{\mu-1}^{1-\eta}E_1(\mho)-t_{\mu-2}^{1-\eta}E_1(\theta)\right]\times\Phi$$
$$+\frac{\alpha(\Delta t)^{\alpha}}{2AB(\alpha)\Gamma(\alpha+3)}\sum_{\mu=2}^{\delta}[t_{\mu}^{1-\eta}E_1(t_\mu,S^\mu,E^\mu,W^\mu,I^\mu,R^\mu)-2t_{\mu-1}^{1-\eta}E_1(\mho)$$
$$-t_{\mu-2}^{1-\eta}E_1(\Theta)]\times\zeta$$

$$W^{\delta+1}=\frac{1-\alpha}{AB(\alpha)}t_{\delta}^{1-\eta}W_1(t_\delta,S^\delta,E^\delta,W^\delta,I^\delta,R^\delta)+\frac{\alpha(\Delta t)^{\mu}}{AB(\alpha)\Gamma(\alpha+1)} \tag{69}$$
$$\sum_{\mu=2}^{\delta}t_{\mu-2}^{1-\eta}W_1(\Theta)\times\Psi+\frac{\alpha(\Delta t)^{\alpha}}{AB(\alpha)\Gamma(\alpha+2)}$$
$$\sum_{\mu=2}^{\delta}\left[t_{\mu-1}^{1-\eta}W_1(\mho)-t_{\mu-2}^{1-\eta}W_1(\theta)\right]\times\Phi$$
$$+\frac{\alpha(\Delta t)^{\alpha}}{2AB(\alpha)\Gamma(\alpha+3)}\sum_{\mu=2}^{\delta}[t_{\mu}^{1-\eta}W_1(t_\mu,S^\mu,E^\mu,W^\mu,I^\mu,R^\mu)-2t_{\mu-1}^{1-\eta}W_1(\mho)$$
$$-t_{\mu-2}^{1-\eta}W_1(\Theta)]\times\zeta$$

$$I^{\delta+1}=\frac{1-\alpha}{AB(\alpha)}t_{\delta}^{1-\eta}I_1(t_\delta,S^\delta,E^\delta,W^\delta,I^\delta,R^\delta)+\frac{\alpha(\Delta t)^{\mu}}{AB(\alpha)\Gamma(\alpha+1)} \tag{70}$$
$$\sum_{\mu=2}^{\delta}t_{\mu-2}^{1-\eta}S_1(\Theta)\times\Psi+\frac{\alpha(\Delta t)^{\alpha}}{AB(\alpha)\Gamma(\alpha+2)}$$
$$\sum_{\mu=2}^{\delta}\left[t_{\mu-1}^{1-\eta}I_1(\mho)-t_{\mu-2}^{1-\eta}I_1(\theta)\right]\times\Phi$$
$$+\frac{\alpha(\Delta t)^{\alpha}}{2AB(\alpha)\Gamma(\alpha+3)}\sum_{\mu=2}^{\delta}[t_{\mu}^{1-\eta}I_1(t_\mu,S^\mu,E^\mu,W^\mu,I^\mu,R^\mu)-2t_{\mu-1}^{1-\eta}I_1(\mho)$$
$$-t_{\mu-2}^{1-\eta}I_1(\Theta)]\times\zeta$$

$$R^{\delta+1}=\frac{1-\alpha}{AB(\alpha)}t_{\delta}^{1-\eta}R_1(t_\delta,S^\delta,E^\delta,W^\delta,I^\delta,R^\delta)+\frac{\alpha(\Delta t)^{\mu}}{AB(\alpha)\Gamma(\alpha+1)} \tag{71}$$
$$\sum_{\mu=2}^{\delta}t_{\mu-2}^{1-\eta}R_1(\Theta)\times\Psi+\frac{\alpha(\Delta t)^{\alpha}}{AB(\alpha)\Gamma(\alpha+2)}$$
$$\sum_{\mu=2}^{\delta}\left[t_{\mu-1}^{1-\eta}R_1(\mho)-t_{\mu-2}^{1-\eta}R_1(\theta)\right]\times\Phi$$
$$+\frac{\alpha(\Delta t)^{\alpha}}{2AB(\alpha)\Gamma(\alpha+3)}\sum_{\mu=2}^{\delta}[t_{\mu}^{1-\eta}R_1(t_\mu,S^\mu,E^\mu,W^\mu,I^\mu,R^\mu)-2t_{\mu-1}^{1-\eta}R_1(\mho)$$
$$-t_{\mu-2}^{1-\eta}R_1(\Theta)]\times\zeta$$

where

$$\Psi=[(\delta-\mu+1)^{\alpha}-(\delta-\mu)^{\alpha}] \tag{72}$$

$$\Theta = t_{\mu-2}, S^{\mu-2}, E^{\mu-2}, W^{\mu-2}, I^{\mu-2}, R^{\mu-2} \tag{73}$$

$$\mho = t_{\mu-1}, S^{\mu-1}, E^{\mu-1}, W^{\mu-1}, I^{\mu-1}, R^{\mu-1} \tag{74}$$

$$\Phi = \left[(\delta-\mu+1)^{\alpha}(\delta-\mu+3+2\alpha) - (\delta-\mu)^{\alpha}(\delta-\mu+3+3\alpha)\right] \tag{75}$$

$$\begin{aligned}\zeta = &\left[(\delta-\mu+1)^{\alpha}\left(2(\delta-\mu)^2+(3\alpha+10)(\delta-\mu)+2\alpha^2+9\alpha+12\right)\right. \\ &\left.-(\delta-\mu)^{\alpha}\left(2(\delta-\mu)^2+(5\alpha+10)(\delta-\mu)+6\alpha^2+18\alpha+12\right)\right]\end{aligned} \tag{76}$$

5 Results and Discussion

The simulation of the taken into-consideration version is depicted inside the figures in this phase the usage of the values of the simple parameters from the simulations of the different classes of COVID-19 SEWIR model with FFM operator are demonstrated in the following Figures for distinct values of fractional order alpha. We consider FFM for the COVID-19 model by using parametric values of α and η. In this part, we talk about numerically simulating the proposed plan for the COVID-19 model using a fractal fractional technique. An analysis of the disease transmission using simulations is given using the COVID-19 SEWIR fractional order model. For this reason, we utilized the COVID-19 model's fractal-fractional derivative in conjunction with the Mittag-Leffler equation with the given beginning circumstances. A nonlinear system's results are found using fractional values.

In figs 1-5 we compare the results of the compartments in Case 1 and Case 2. In Case 1, we take $m = 0.35$ and $k1 = 0.3$. Then, $R_0 = 8.1769 > 1$ and $P^*(E^*, I^*, S^*, W^*) = (7.2730, 6.1898, 2.7730, 2.4516)$. In a similar manner, the population size under the circumstance $R_0 > 1$ is also simulated. The relative outcomes are shown. In Case 2, we take $m = 0.8$ and $k_1 = 0.6$. Then, $R_0 = 0.9802 < 1$ and $P_0(0, 0, S0, 0) = (0, 0, 3.4091, 0)$. Then, under the assumption that $R_0 < 1$, we model changes in the numbers of these four populations. Conclusion: A shorter length of the epidemic is caused by a drop in the starting value of vulnerable people at the start of the outbreak. While this is happening, a lower level is reached by the peak of verified cases very immediately. Although around 20 days later than in Case 2, the number of the four communities in Case 1 begins to stabilize about day 160. The pandemic will continue in Case 1 since neither the exposure nor the afflicted communities can completely vanish. But as seen in Case 1, once the four communities have stabilized, the whole community will be made up of the vaccinated susceptible and recovered community. This goal for epidemic control is of top importance. Similar amounts of time are used by the exposed and infected communities in Cases 1 and 2, although Case 1's peak is greater. Therefore, we may conclude from these results that both government engagement and vaccination have an effect on the dynamics of the epidemic. The results of the research above indicate that m and k_1 both contribute to the prevention and management of the pandemic. As a result, we will particularly research how well m and k_1 work to regulate COVID-19. The starting point is (120, 0, 15, 1, 0). We will note changes in the populations exposed to the quarantined virus W(t) and I(t), respectively. Fractional order derivations, which might be the most outstanding and dependable compared to classical order, were greater efficient in explaining bodily approaches. In contrast, those operators are extra worthwhile than current non-integer order fashions. The supplied numerical results represent the conduct of the dynamics that may be observed within the one-of-a-kind fractal orders.

6 Conclusion

Mathematical modeling plays a crucial role in manipulating, preparing for, and navigating the terrible impacts of infectious illnesses on society via historical decline. The outcome of the fractional order version has a memory impact on the fashionable version, in contrast to the classical version. Critiques of the suggested strategy that are both qualitative and quantitative are also explored. The analysis of the fractal fractional operators is further explored in great depth. Additionally, utilizing the Mittag-Leffler Kernel, we developed a numerical simulation of a kind of fractional differential equations. We utilized Matlab to simulate the consequences for extremely high fractional order and fractal size values. We've seen that the ground-breaking operator yields excellent results even when used in the mathematical modeling of the COVID-19 SEWIR model. The figures show that changing the fractal order has an impact on how the recommended model behaves. The illustrations show how fractal and fractional orders interact. We discover that the suggested model is effectively useable as a modeling tool and also offers insight into the dynamics of disturbances thanks to the graphical impact. The fractional order analyzes the frame in which the diseased character is comprised of diseases from the beginning to the conclusion, as opposed to the non-integer order derivation, which analyzes the illness in one section unambiguously. It makes it easier to study the entire behavior of COVID-19 use from beginning to end. The results of this study can help by giving information to policy-makers and public health professionals so that they can stop the spread of COVID-19.

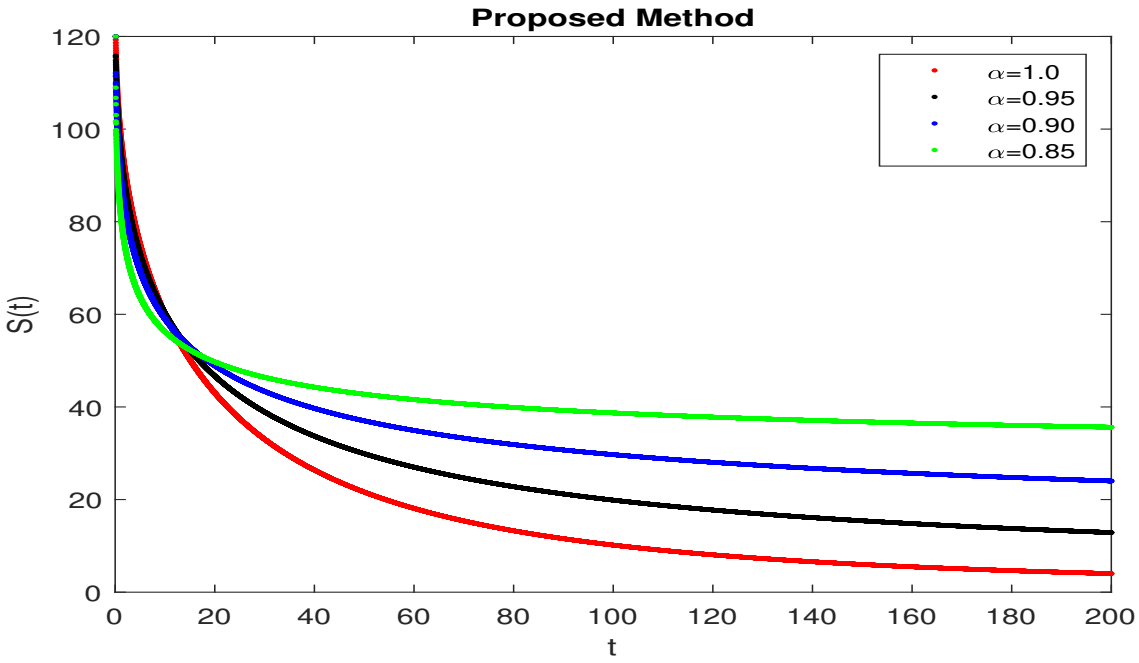

Case-1 with $m = 0.35$ and $k_1 = 0.2$

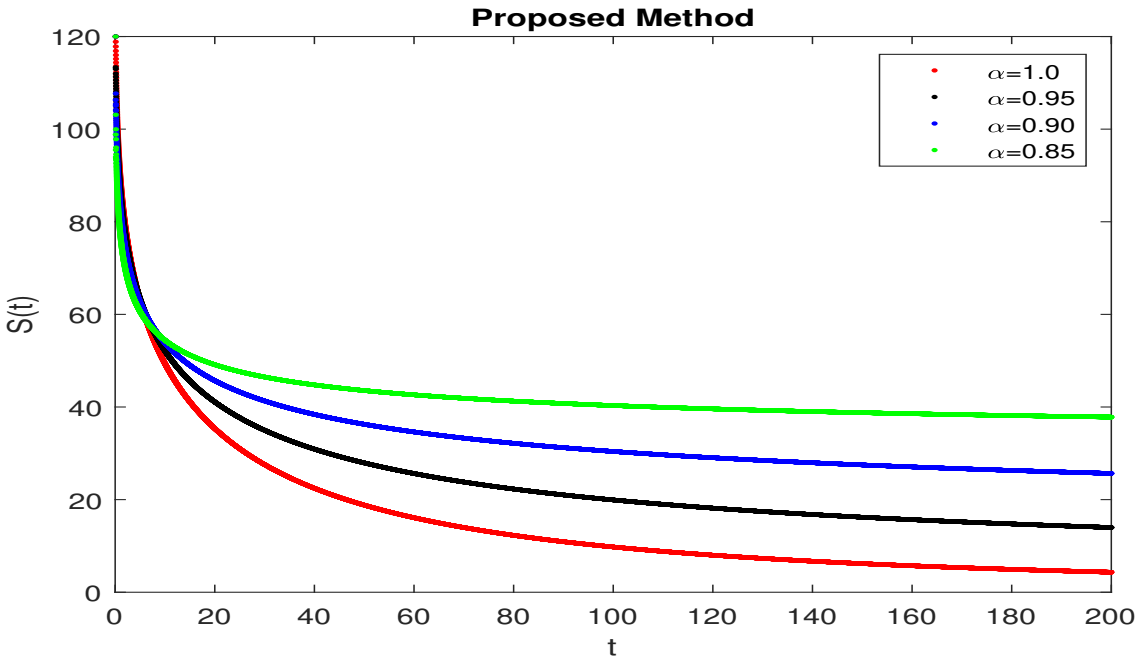

Case-2 with $m = 0.8$ and $k_1 = 0.6$

Fig. 1: Simulation of segment S(t) under fractal-fractional

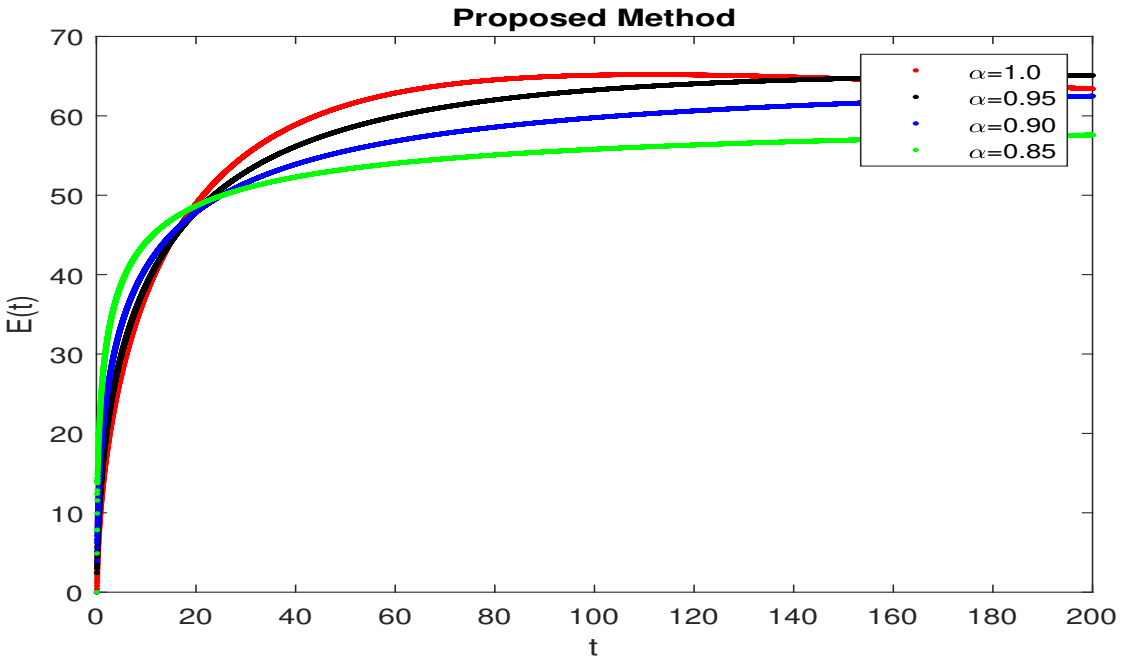

Case-1 with $m = 0.35$ and $k_1 = 0.2$

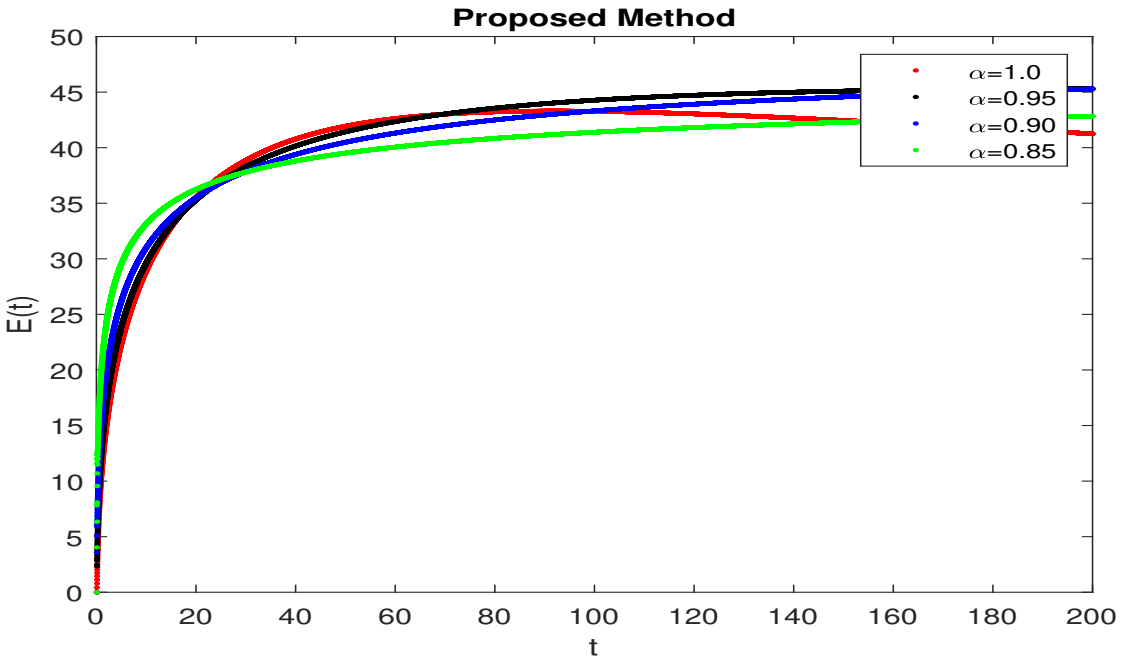

Case-2 with $m = 0.8$ and $k_1 = 0.6$

Fig. 2: Simulation of segment E(t) under fractal-fractional

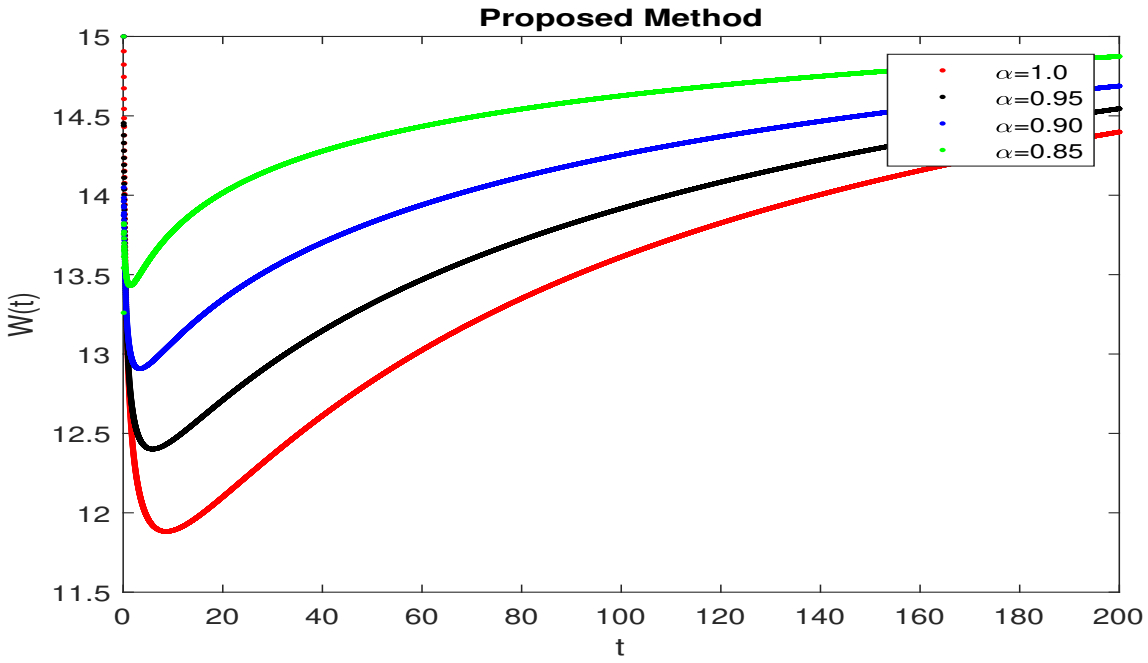

Case-1 with $m = 0.35$ and $k_1 = 0.2$

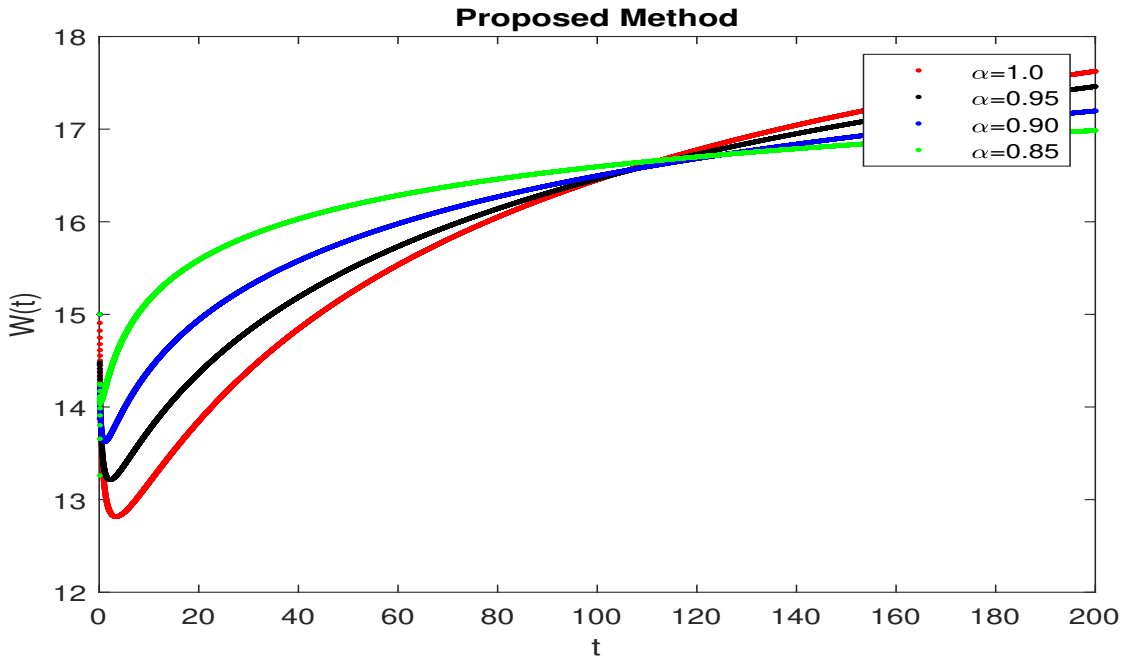

Case-2 with $m = 0.8$ and $k_1 = 0.6$

Fig. 3: Simulation of segment W(t) under fractal-fractional

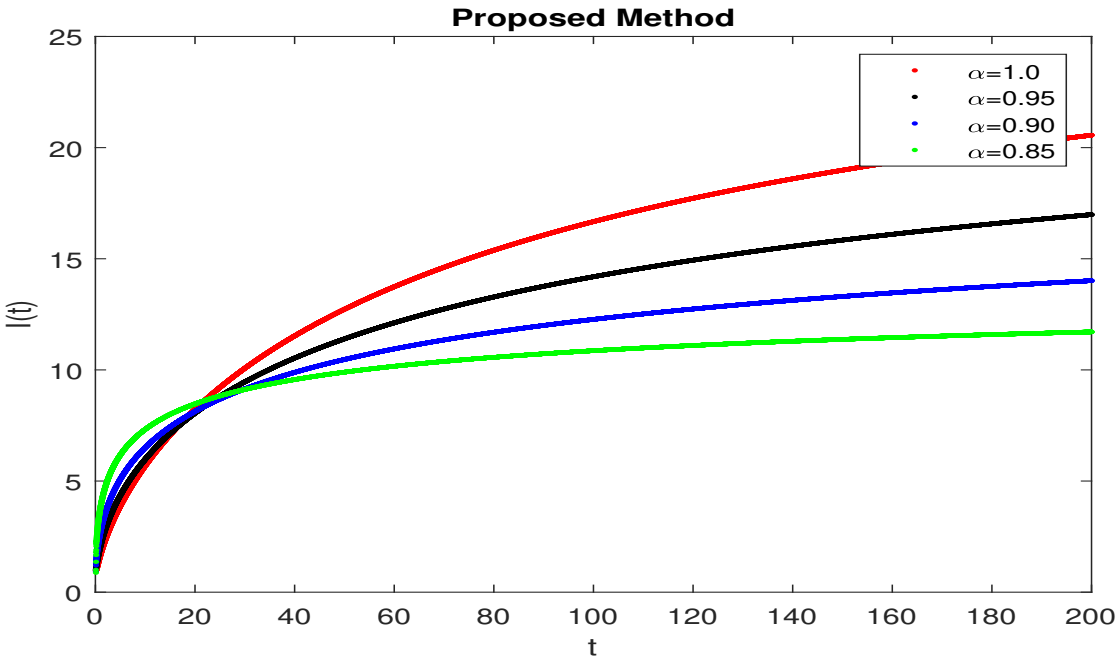

Case-1 with $m = 0.35$ and $k_1 = 0.2$

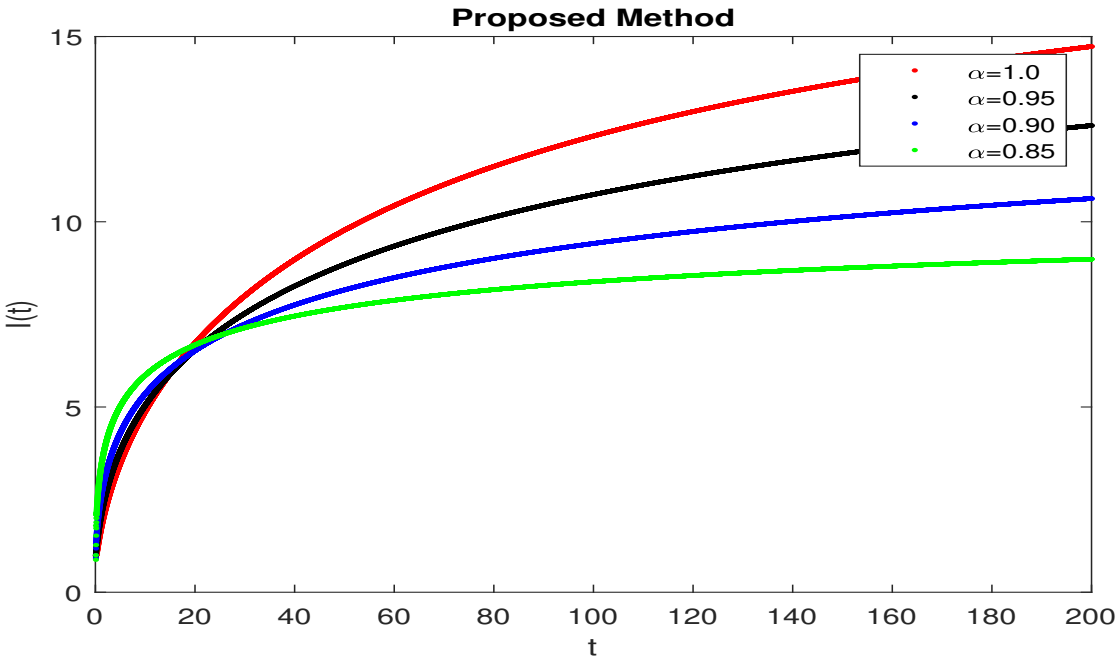

Case-2 with $m = 0.8$ and $k_1 = 0.6$

Fig. 4: Simulation of segment I(t) under fractal-fractional

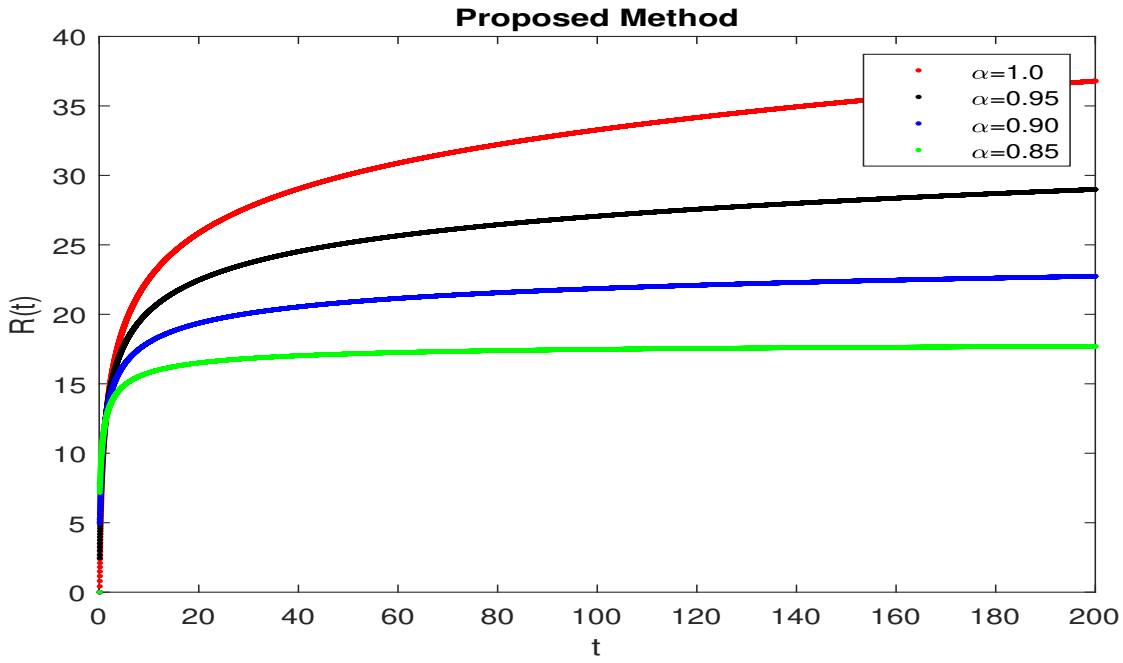

Case-1 with $m = 0.35$ and $k_1 = 0.2$

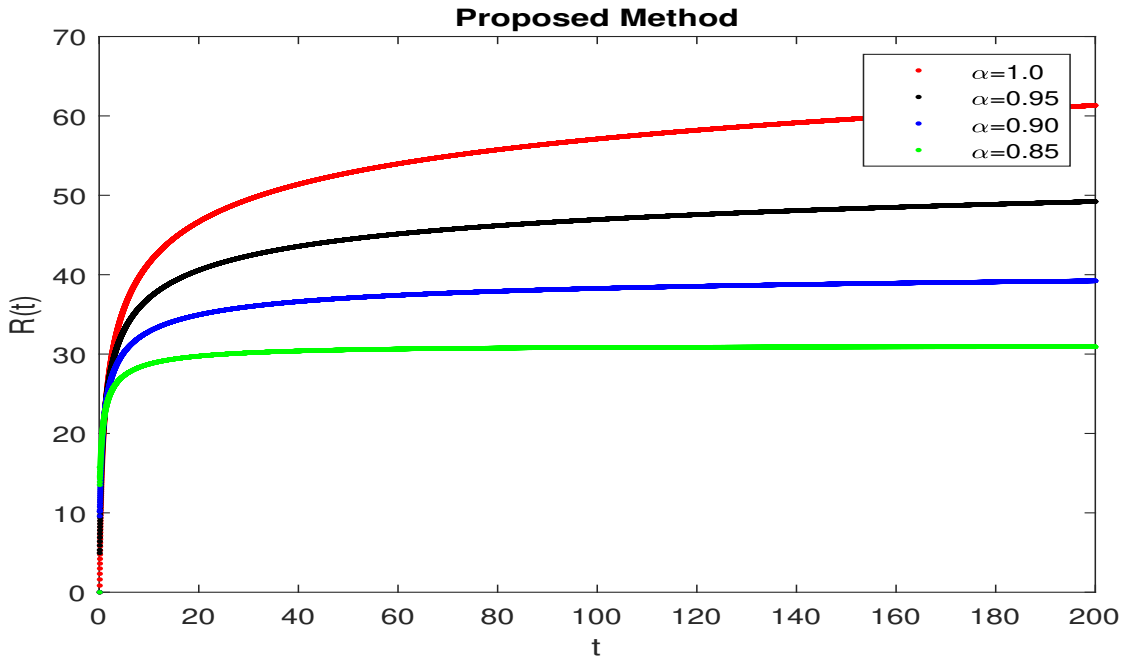

Case-2 with $m = 0.8$ and $k_1 = 0.6$

Fig. 5: Simulation of segment R(t) under fractal-fractional

References

[1] Zheng, Y. Y., Ma, Y. T., Zhang, J. Y., and Xie, X. (2020). COVID-19 and the cardiovascular system. Nature reviews cardiology, 17(5), 259-260.

[2] Long, A., and Ascent, D. (2020). World economic outlook. International Monetary Fund, 177.

[3] Vo, T. D., and Tran, M. D. (2021). The impact of covid-19 pandemic on the global trade. International Journal of Social Science and Economics Invention, 7(1), 1-7.

[4] Dayour, F., and Adam, I. (2022). Entrepreneurial motivations among COVID-19 induced redundant employees in the hospitality and tourism industry. Journal of Human resources in Hospitality and tourism, 21(1), 130-155.

[5] Almeida, R. (2018). Analysis of a fractional SEIR model with treatment. Applied Mathematics Letters, 84, 56-62.

[6] Carcione, J. M., Santos, J. E., Bagaini, C., and Ba, J. (2020). A simulation of a COVID-19 epidemic based on a deterministic SEIR model. Frontiers in public health, 8, 230.

[7] Caputo, M. (1967). Linear models of dissipation whose Q is almost frequency independent-II. Geophysical Journal International, 13(5), 529-539.

[8] Li, Z., Liu, Z., and Khan, M. A. (2020). Fractional investigation of bank data with fractal-fractional Caputo derivative. Chaos, Solitons and Fractals, 131, 109528.

[9] Chen, W., Sun, H., Zhang, X., and Koroak, D. (2010). Anomalous diffusion modeling by fractal and fractional derivatives. Computers and Mathematics with Applications, 59(5), 1754-1758.

[10] Kober, H. (1940). On fractional integrals and derivatives, Quart. J. Maths. Oxford, 193-211.

[11] Holm, S., and Näsholm, S. P. (2011). A causal and fractional all-frequency wave equation for lossy media. The Journal of the Acoustical Society of America, 130(4), 2195-2202.

[12] Atangana, A., and Baleanu, D. (2016). New fractional derivatives with nonlocal and non-singular kernel: theory and application to heat transfer model. arXiv preprint arXiv:1602.03408.

[13] Atangana, A. (2017). Fractal-fractional differentiation and integration: connecting fractal calculus and fractional calculus to predict complex system. Chaos, solitons and fractals, 102, 396-406.

[14] Farman, M., Akgül, A., Tekin, M. T., Akram, M. M., Ahmad, A., Mahmoud, E. E., and Yahia, I. S. (2022). Fractal fractional-order derivative for HIV/AIDS model with Mittag-Leffler kernel. Alexandria Engineering Journal, 61(12), 10965-10980.

[15] Farman, M., Hasan, A., Sultan, M., Ahmad, A., Akgül, A., Chaudhry, F., ... and Weera, W. (2022). Yellow virus epidemiological analysis in red chili plants using Mittag-Leffler kernel. Alexandria Engineering Journal.

[16] Farman, M., Akgül, A., Abdeljawad, T., Naik, P. A., Bukhari, N., and Ahmad, A. (2022). Modeling and analysis of fractional order Ebola virus model with Mittag-Leffler kernel. Alexandria Engineering Journal, 61(3), 2062-2073.

[17] Tabassum, M. F., Khan, S., Farman, M., Umer, M., Saleem, A. S. A., Ahmad, A., and ul Hassan, S. M. Glucose Insulin Algorithm for for Artificial Pancreas to Control the Type 1 Diabetes Mellitus

[18] Farman, M., Akgül, A., Ahmad, A., and Imtiaz, S. (2020). Analysis and dynamical behavior of fractional-order cancer model with vaccine strategy. Mathematical Methods in the Applied Sciences, 43(7), 4871-4882.

[19] Carey, K. B. (1995). Heavy drinking contexts and indices of problem drinking among college students. Journal of Studies on Alcohol, 56(3), 287-292.

[20] Gonzalez, V. M., Collins, R. L., and Bradizza, C. M. (2009). Solitary and social heavy drinking, suicidal ideation, and drinking motives in underage college drinkers. Addictive Behaviors, 34(12), 993-999.

[21] Scholte, R. H., Poelen, E. A., Willemsen, G., Boomsma, D. I., and Engels, R. C. (2008). Relative risks of adolescent and young adult alcohol use: The role of drinking fathers, mothers, siblings, and friends. Addictive behaviors, 33(1), 1-14.

[22] Adu, I. K., Osman, M. A. R. E. N., and Yang, C. (2017). Mathematical model of drinking epidemic. Br. J. Math. Computer Sci, 22(5).

[23] Huo, H. F., Huang, S. R., Wang, X. Y., and Xiang, H. (2017). Optimal control of a social epidemic model with media coverage. Journal of Biological Dynamics, 11(1), 226-243.

[24] Huo, H. F., and Song, N. N. (2012). Global stability for a binge drinking model with two stages. Discrete Dynamics in Nature and Society, 2012.

[25] Wang, X. Y., Huo, H. F., Kong, Q. K., and Shi, W. X. (2014, January). Optimal control strategies in an alcoholism model. In Abstract and Applied Analysis (Vol. 2014). Hindawi.

[26] Young-Wolff, K. C., Wang, P., Tuvblad, C., Baker, L. A., Raine, A., and Prescott, C. A. (2015). Drinking experience uncovers genetic influences on alcohol expectancies across adolescence. Addiction, 110(4), 610-618.

[27] Farman, M. (2022). Fractional order SIR and SEIR models for COVID-19 with saturating incidence rate. Communications in Nonlinear Science and Numerical Simulation, 98, 105261.

[28] Haq, I. U., Ali, N., Ahmad, H., Sabra, R., Albalwi, M. D., and Ahmad, I. (2023). Mathematical analysis of a Corona virus model with Caputo, Caputo-Fabrizio-Caputo fractional and Atangana-Baleanu-Caputo differential operators. International Journal of Biomathematics.

[29] Almutairi, N., Saber, S., and Ahmad, H. (2023). The fractal-fractional Atangana-Baleanu operator for pneumonia disease: stability, statistical and numerical analyses. AIMS Mathematics, 8(12), 29382-29410.

[30] Ahmad, H., Khan, M. N., Ahmad, I., Omri, M., and Alotaibi, M. F. (2023). A meshless method for numerical solutions of linear and nonlinear time-fractional Black-Scholes models. AIMS Mathematics, 8(8), 19677-19698.

[31] Ahmad, H., Ozsahin, D. U., Farooq, U., Fahmy, M. A., Albalwi, M. D., and Abu-Zinadah, H. (2023). Comparative analysis of new approximate analytical method and Mohand variational transform method for the solution of wave-like equations with variable coefficients. Results in Physics, 106623.
[32] Al-Refai, M., and Baleanu, D. (2022). On an extension of the operator with Mittag-Leffler kernel. Fractals, 30(05), 2240129.
[33] Baleanu, D., Fernandez, A., and Akgül, A. (2020). On a fractional operator combining proportional and classical differintegrals. Mathematics, 8(3), 360.
[34] Xu, C., Liao, M., Li, P., Guo, Y., Xiao, Q., and Yuan, S. (2019). Influence of multiple time delays on bifurcation of fractional-order neural networks. Applied Mathematics and Computation, 361, 565-582.
[35] Xu, C., Zhang, W., Liu, Z., and Yao, L. (2022). Delay-induced periodic oscillation for fractional-order neural networks with mixed delays. Neurocomputing, 488, 681-693.
[36] Hasan, A., Akgül, A., Farman, M., Chaudhry, F., Sultan, M., and De la Sen, M. (2023). Epidemiological Analysis of Symmetry in Transmission of the Ebola Virus with Power Law Kernel. Symmetry, 15(3), 665.
[37] Sajjad, A., Farman, M., Hasan, A., and Nisar, K. S. (2023). Transmission dynamics of fractional order yellow virus in red chili plants with the Caputo Fabrizio operator. Mathematics and Computers in Simulation, 207, 347-368.
[38] Huang, W. H., Samraiz, M., Mehmood, A., Baleanu, D., Rahman, G., and Naheed, S. (2023). Modified Atangana-Baleanu fractional operators involving generalized Mittag-Leffler function. Alexandria Engineering Journal, 75, 639-648.
[39] ur Rahman, M., Arfan, M., and Baleanu, D. (2023). Piecewise fractional analysis of the migration effect in plant-pathogen-herbivore interactions. Bulletin of Biomathematics, 1(1), 1-23.
[40] Alijani, Z., Shiri, B., Perfilieva, I., and Baleanu, D. (2023). Numerical solution of a new mathematical model for intravenous drug administration. Evolutionary Intelligence, 1-17.
[41] Bozkurt, F., Yousef, A., Bilgil, H., and Baleanu, D. (2023). A mathematical model with piecewise constant arguments of colorectal cancer with chemo-immunotherapy. Chaos, Solitons and Fractals, 168, 113207.
[42] Umapathy, K., Palanivelu, B., Jayaraj, R., Baleanu, D., and Dhandapani, P. B. (2023). On the decomposition and analysis of novel simultaneous SEIQR epidemic model. AIMS Mathematics, 8(3), 5918-5933.
[43] Jajarmi, A., and Baleanu, D. (2018). A new fractional analysis on the interaction of HIV with CD4+ T-cells. Chaos, Solitons and Fractals, 113, 221-229.
[44] Farman, M. (2021). A fractional order SIR model for COVID-19 epidemic with time-varying parameters. Applied Mathematics and Computation, 403, 126410.
[45] Farman, M. (2021). A fractional order SEIR model for COVID-19 transmission dynamics. Chaos, Solitons and Fractals, 140, 110099.
[46] Xiang, H., Zhu, C. C., and Huo, H. F. (2017). Modelling the effect of immigration on drinking behaviour. Journal of biological dynamics, 11(1), 275-298.
[47] Jiayi, L., Sixian, L., Weixuan, S., Manfeng, H., and Jingxiang, Z. (2022). Optimal Control and Stability Analysis of an SEIR Model with Infectious Force in Latent Period. Computational Intelligence and Neuroscience, 2022.
[48] Iqbal, Z., Macías-Díaz, J. E., Ahmed, N., Javaid, A., Rafiq, M., and Raza, A. (2022). Analytical and Numerical Boundedness of a Model with Memory Effects for the Spreading of Infectious Diseases. Symmetry, 14(12), 2540.
[49] Ahmad S., Ullah A., Abdeljawad T., Akgül A., Mlaiki N. (2021). Analysis of fractal-fractional model of tumor-immune interaction, Results in Physics, 25, 104178.
[50] Xu, C.; Farman, M.; Hasan, A.; Akgül, A.; Zakarya, M.; Albalawi, W.; Park, C. Lyapunov Stability and Wave Analysis of COVID-19 Omicron Variant of Real Data with Fractional Operator. Alexandria Engineering Journal, 2022, 61, 11787-11802.